Doctor of Philosophy

Aryl Hydrocarbon Receptor Antagonists Alleviate Acute Hepatic Ischemia-Reperfusion Injury

The Graduate School
of the University of Ulsan
Department of Medical Science
Jae-Im Kwon

Aryl Hydrocarbon Receptor Antagonists Alleviate Acute Hepatic Ischemia-Reperfusion Injury

Supervisor: Dong Cheol Woo

A Dissertation

Submitted to
The Graduate School of the University of Ulsan
In partial Fulfillment of the Requirements
For the Degree of

Doctor of Philosophy

by

Jae-Im Kwon

Department of Medical Science
University of Ulsan, Korea
February 2024

Aryl Hydrocarbon Receptor Antagonists Alleviate Acute Hepatic Ischemia-Reperfusion Injury

This certifies that the dissertation of Jae-Im Kwon is approved.

_____

Committee Chair Dr. Kyung Won Kim

_____

Committee Member Dr. Jeong Kon Kim

_____

Committee Member Dr. Dong Cheol Woo

_____

Committee Member Dr. In-Jeoung Baek

_____

Committee Member Dr. C-Yoon Kim

Department of Medical Science

University of Ulsan, Korea

February 2024

Contents

CONTENTS OF TABLES AND FIGURES

Abstract

Aryl hydrocarbon receptors (AhRs) are important mediators of ischemic injury in the brain. Furthermore, pharmacological inhibition of AhR activation after ischemia attenuates cerebral ischemia-reperfusion (IR) injury. Here, we investigated whether administration of an AhR antagonist after ischemia was effective in ameliorating hepatic IR injury. Therefore, a 70% partial hepatic IR injury (45-min ischemia and 24-h reperfusion) was induced in rats, and 6,2',4'-trimethoxyflavone (TMF; 5 mg/kg) was administered to them intraperitoneally 10 min after ischemia. Hepatic IR injury was assed using serum samples, magnetic resonance imaging-based liver function indices, and liver samples. TMF-treated rats showed significantly lower relative enhancement (RE) values and serum alanine aminotransferase (ALT) and aspartate aminotransferase levels than control rats 3 h after reperfusion. Additionally, 24 h after reperfusion, TMF-treated rats had significantly lower RE values, ΔT1 values, serum ALT levels, and necrotic area percentage than rats of the control group. Moreover, the expression of the apoptosis-related proteins Bax and cleaved caspase-3 was significantly lower in TMF-treated rats than in control rats. This study showed that AhR activation inhibition after ischemia ameliorates IR-induced liver injury in rats.

Key words: Aryl hydrocarbon receptor, hepatic ischemia-reperfusion injury, magnetic resonance imaging

ABBREVIATION

AhR, aryl hydrocarbon receptor

IR, ischemia-reperfusion

TMF, 6,2',4'-trimethoxyflavone

RE, relative enhancement

ALT, alanine aminotransferase

KC, kupffer cells

L-Kyn, L-kynurenine

TDO, tryptophan-2,3-dioxygenase

MRI, magnetic resonance imaging

Sis, signal intensities

T1 Wis, T1-weighted gradient echo images

AST, aspartate aminotransferase

TUNEL, terminal deoxynucleotidyl transferase-mediated dUTP nick-end labeling

C-cas, cleaved caspase-3

LC-MS/MS, Liquid chromatography-tandem mass spectrometry

OATB1B1/B3, organic anion transporting polypeptide

DMSO, dimethyl sulfoxide

ROI, regions of interest

H&E, hematoxylin and eosin

SDS-PAGE, sodium dodecyl sulfate-polyacrylamide gel electrophoresis

PVDF, polyvinylidene fluoride

HRP, horseradish peroxidase

IHC, immunohistochemistry

RNA, ribonucleic acid

qRT PCR, quantitative real time PCR

I. Introduction

Hepatic ischemia-reperfusion (IR) injury commonly occurs during liver transplantation or resection and is considered a leading cause of liver damage and dysfunction.[1–5] Though the mechanisms that underlie such hepatic IR injury have been extensively investigated, they are still unclear. Furthermore, it is known that hepatic IR injury involves anaerobic metabolism, mitochondria, oxidative stress, intracellular calcium overload, liver Kupffer cells (KC), neutrophils, cytokines, and chemokines, but, in clinical practice, effective prevention and treatments are still lacking.[6]

The aryl hydrocarbon receptor (AhR) is a ligand-activated basic helix-loop-helix/Per-ARNT-Sim transcription factor that mediates the toxic and carcinogenic effects of xenobiotics.[7,8] Upon ligand binding, AhR translocates to the nucleus to form an active heterodimeric complex. This complex triggers rapid transcriptional activations in several organs and cellular systems.[9] Recent studies have suggested that, during cerebral ischemia, L-kynurenine (L-Kyn) —an endogenous ligand of AhR— is accumulated in the brain, triggering AhR activation and exacerbating neuronal damage.[10,11] Moreover, *in vivo* experiments have demonstrated that the pharmacological manipulation of AhR activation after ischemia modulates neuronal damage due to cerebral IR.[12] Brain observations suggest that similar pathways may be involved in the liver. Since L-Kyn is produced in significant amounts in the liver through the degradation of L-tryptophan by tryptophan-2,3-dioxygenase (TDO),[13] it may accumulate in the liver more easily than in the brain after ischemia. Consequently, ischemia-induced AhR activation and tissue damage after reperfusion may be greater in the liver than in the brain, and AhR activation inhibition after ischemia might be effective in suppressing hepatic IR injury. However, to the best of our knowledge, the effects of AhR antagonism on hepatic IR have not yet been reported.

In this study, we investigated the protective effects of AhR antagonism after ischemia in a murine model of hepatic IR injury. Moreover, we used *in vivo* magnetic resonance imaging (MRI) and molecular biology techniques to evaluate whether the administration of an AhR antagonist could have hepatoprotective effects.

II. Materials and Method

II-1. Ethics statements

This study was approved by the Institutional Animal Care and Use Committee of Asan Medical Center (IACUC Number: 2019-02-035). Procedures were performed in strict accordance with the guidelines of the Association for Assessment and Accreditation of Laboratory Animal Care. The experiments were reported in accordance with the Animal Research: Reporting *in Vivo* Experiments (ARRIVE) guidelines on how to report animal experiments. All animal surgeries were performed under isoflurane anesthesia and closely monitored by trained individuals capable of assessing pain-related behaviors. Euthanasia was planned if the animals exhibited persistent pain-related behaviors; however, none of them exhibited severe pain-related behaviors during the experimental period.

II-2. Partial (70%) hepatic IR injury model

Sprague-Dawley rats (8-week-old males; weight range: 290–310 g; Orient Bio, Pyeongtaek, Republic of Korea) were used in the experiments. Rats were housed in cages, three per cage, under a 12 h light/12 h dark cycle at a constant temperature (24–25 ℃). Rats received food and water *ad libitum*.

Based on previous studies, a 70% partial hepatic IR injury model was established in the rats.[4,25] Briefly, the abdominal cavity was exposed by a midline incision and the portal triad (hepatic artery, portal vein, and bile duct), which supplied the left lateral and median lobes, was clamped (Fig. 5). The clamp was removed 45 min after the development of ischemia, and the abdomen was closed in a single layer. Successful induction of hepatic ischemia was visually confirmed by observing the median and left lobes of the liver, which turned pale compared to the non-ischemic lobes (right and caudate lobes). Successful reperfusion was also determined by the color of the ischemic lobes, which returned to their original color (that of the non-ischemic lobes). All rats were initially anesthetized with 5% isoflurane in 70% N_2O/30% O_2 (flow rate, 1.0 L/min), and anesthesia was maintained with 2% isoflurane during surgery.

II-3. Drug treatment

TMF (Sigma-Aldrich, St. Louis, MO, USA), the AhR antagonist, was dissolved in dimethyl sulfoxide (DMSO; Sigma-Aldrich) and used at a concentration of 5 mg/kg.[12] Equal volumes of DMSO were used in the vehicle-treated control group. All the treatments were administered via intraperitoneal injection.

II-4. Animal groups

The rats were randomly divided into the following groups: (1) Sham group: rats with no IR modeling or vehicle injection (n = 8), (2) control group: rats with IR

modeling and vehicle injection (n = 8), and (3) TMF group: rats with IR modeling and drug administration 10 min after ischemia (n = 8).

II-5. MRI

MRI was performed using a 9.4 T MRI system (Agilent Technologies, Santa Clara, CA, USA) and a 63-mm transmit/receive volume coil. The animals were kept under respiratory anesthesia with 2.0–2.5% isoflurane in a 1:2 mixture of O_2:N_2O at a constant body temperature of 37.5 ± 0.5 ℃ (through an air heater system) during image acquisition. Rats were continuously monitored for stable breathing.

MRI data were obtained 3 and 24 h after reperfusion. MRI protocols included T1-WI and T1 mapping. The parameters of each sequence are listed in Supplementary Table S1. MRI images were obtained before and 20 min after the administration of Gd-EOB-DTPA (25 μM/kg; Primovist, Bayer Korea, South Korea).[22]

II-6. MRI analysis

All MRI data were analyzed using ImageJ (National Institutes of Health, Bethesda, MA, USA; https://rsbweb.nih.gov/ij/) by an observer blinded to the grouping information. The mean SI values and T1 relaxation times were measured on T1-WIs and T1 maps obtained before and 20 min after Gd-EOB-DTPA administration. Regions of interest (ROIs) were manually placed at identical locations on the hepatic parenchyma and paravertebral muscle on the T1-WIs and T1 maps. ROIs were placed on the hepatic parenchyma to avoid visible blood vessels or imaging artifacts. Two ROIs were randomly placed in the liver and paravertebral muscles on the T1-WIs and T1 maps before and after Gd-EOB-DTPA administration (Fig. 3). The mean SI and T1 values for both ROIs in the liver were considered representative of the SI and T1 values for the entire liver, respectively. The mean SI values for both ROIs in the paravertebral muscle were regarded as representative SI values for the entire paravertebral muscle. The size of the ROIs ranged from 10 to 11 mm^2 in the liver parenchyma and from 8 to 9 mm^2 in the paravertebral muscles. MRI-based liver function indices were calculated from the SI measurements or T1 relaxation time before ($SI\text{-}_{pre}$, $T1\text{-}_{pre}$) and 20 min after ($SI\text{-}_{post}$, $T1\text{-}_{post}$) Gd-EOB-DTPA administration as follows: (1) RE of the liver = $(SI\text{-}_{post} - SI\text{-}_{pre})/SI\text{-}_{pre}$; (2) LMR = $SI\text{-}_{post}$ of the liver/$SI\text{-}_{post}$ of the muscle; (3) $T1\text{-}_{post}$ = $T1\text{-}_{post}$ values of the liver; and (4) $\Delta T1 = T1\text{-}_{pre} - T1\text{-}_{post}$.[23,24]

II-7. Measurement of serum enzymes

Blood samples were obtained from the jugular vein of the rats 3 and 24 h after reperfusion. The samples were centrifuged at 2,000 rpm for 14 min to obtain serum for analysis. Serum ALT and AST activities were determined using a biochemical analyzer (7180, Hitachi, Tokyo, Japan).

II-8. Hematoxylin and eosin (H&E) staining

Liver tissues were harvested 24 h after reperfusion and fixed in 4% paraformaldehyde (Biosesang, Seongnam, Republic of Korea). Fixed tissues were embedded in paraffin and sectioned to 3-μm thickness. H&E staining was performed using an automated stainer (Leica, Wetzlar, Germany). The percentage of necrotic areas in five random sections per slide was analyzed under a Vectra microscope (PerkinElmer, MA, USA) at 50×.[26]

II-9. TUNEL assay

A TUNEL assay was performed to detect apoptotic cells using an apoptosis detection kit (Millipore, Billerica, MA, USA) according to the manufacturer's instructions. Paraffin-embedded liver tissue sections were treated with a mixture of reaction buffer and enzyme (7:3) at 37 ℃ for 1 h, and the anti-digoxigenin peroxidase conjugate was treated at room temperature for 30 minutes. The tissue was then treated with DAB substrate (3,3' diaminobenzidine tetrahydrochloride hydrate, Sigma-Aldrich) (1:50) in the dark for 5 min and stained with hematoxylin (Sigma-Aldrich) for 2 min in the dark. TUNEL-positive cells were observed under a Vectra microscope (PerkinElmer) at 200×.

II-10. Western blotting

Liver tissues from the sham (5 mg), control (30 mg), and TMF groups (30 mg) were centrifuged in cold-PBS at 500 *x g* and at 4 ℃ for 5 min and homogenized in radio-immunoprecipitation (RIPA) buffer (Sigma-Aldrich, MO, USA) with 1× protease inhibitor cocktail (Sigma-Aldrich) on ice. After 30 min, the lysates were centrifuged at 13,000 rpm at 4 ℃ for 20 min. The supernatants were aliquoted into 1.5-mL tubes and quantified using a bicinchoninic acid assay kit (Thermo Fisher Scientific, MA, USA). In total, 30 μg of protein was separated using 8% sodium dodecyl sulfate-polyacrylamide gel electrophoresis (SDS-PAGE) (Thermo Fisher Scientific) and transferred onto a polyvinylidene fluoride (PVDF) membrane (Thermo Fisher Scientific). The membrane was blocked with 5% skim milk (Becton and Dickinson [BD], NJ, USA) in 1× tris-buffered saline (Elpis-Biotech, Daejeon, Republic of Korea) with Tween 20 (Sigma-Aldrich) (TBST) at room temperature for 1 h and then incubated with mouse anti-AhR (1:1000, Santa Cruz Biotechnology, TX, USA), rabbit anti-Bcl-2 (1:1000, Novus Biologicals, CO, USA), rabbit anti-Bax (1:1000, Cell Signaling Technology, MA, USA), rabbit anti-cleaved caspase-3 (C-cas3, 1:1000, Cell Signaling Technology), and mouse anti-GAPDH (1:10000, Thermo Fisher Scientific) at 4 ℃ overnight. The antibodies were washed three times for 10 min in 1 × TBST, and the membrane was incubated with goat anti-mouse (1:5000, Thermo Fisher Scientific) or rabbit (1:2000, Thermo Fisher Scientific) immunoglobulin G secondary antibody-horseradish peroxidase (HRP) conjugate at room temperature for 1 h. The membrane was incubated with Lumi Femto Solution

A:B (A:B = 1:1, DoGenBio, Seoul, Republic of Korea) using a chemiluminescence (ECL) reagent after washing, and AhR was quantified using ImageJ software and GAPDH as reference.

II-11. Immunohistochemistry (IHC) staining

IHC staining was performed using the ultraView universal DAB detection kit (Ventana Medical Systems, Inc., Oro Valley, AZ, USA). The slides were incubated at 60 ℃ for 4 min, EzPrep was used for deparaffinization, and slides were rinsed with Tris buffer (pH 7.6). After placing the slides into the antigen retrieval buffer for 1 h at 100 ℃, they were treated with rabbit anti-AhR (1:1000, Enzo Life Sciences, NY, USA) for 36 min at 37 ℃. Slides were then rinsed and processed with the DISCOVERY Ultra Map anti rabbit HRP for 12 min at 37 ℃. UltraView DAB and DAB H_2O_2 detection kits were used to treat slides for 8 min at 37 ℃; during this time, AhR-positive cells were stained brown. Slides were washed and treated with ultraView COPPER for 4 min at 37 ℃. The slides were rinsed, incubated in hematoxylin for 4 min at 37 ℃, rinsed again, exposed to BLUING REAGENT for 4 min at 37 ℃, and washed. AhR-positive cells were observed under a Vectra microscope at 200× (PerkinElmer).

II-12. qRT PCR

To detect ribonucleic acid (RNA), I/R injury region of hepatic tissue was harvested at 24 h after reperfusion. Total RNA was extracted from hepatic tissue using TRIZOL (Invitrogen, MA, USA). Reverse transcription was performed through cDNA synthesis kit (TAKARA Bio, Otsu, JP). Quantitative real time PCR (qRT PCR) was carried out using SYBR Green PCR Master Mix (Thermo Fisher Scientific, MA, USA) to detect the expressions of AhRR, CYP1a1, CYP1b1, IDO1, IDO2, TDO and GAPDH with primers (Supplementary Table S2).

II-13. LC-MS/MS

Liver tissues were harvested at 24 h after reperfusion. L-Kyn and tryptophan standards, internal standard, and derivatization reagents were purchased from Sigma-Aldrich or CDN isotopes. All solvents including water were purchased from J. T. Baker.

90 – 100 mg of rat hepatic tissues were homogenized using a Tissue-Lyser (Qiagen, Hilden, Germany) with 800 μL chloroform/methanol (2/1, v/v), and the homogenate was incubated at 4 ℃ for 15 min. An internal standard solution containing tryptophan-d_5 was added to reach final concentration to 2 μM and mixed well. Samples were centrifuged at 14,000 rpm for 15 min. The supernatant was collected and 200 μL each of H_2O and chloroform was added. Samples were mixed vigorously and centrifuged at 4,000 rpm for 20 min. Then, aqueous phase was

collected and used for chemical derivatization of amino acids using phenylisothiocyante (PITC). After the reaction, the derivatized amino acids were extracted with 5 mM ammonium acetate in methanol, and ready for LC-MS/MS analysis.

L-Kyn and tryptophan were measured with LC-MS/MS equipped with 1290 HPLC (Agilent, Waldbronn, Germany), 5500 mass spectrometry (Sciex, Toronto, Canada), and a reverse phase column (Zorbax Eclipse XDB-C18 100 × 2mm). 10 μL was injected into the LC-MS/MS system and ionized with turbo spray ionization source. 0.2 % formic acid in H_2O and 0.2 % formic acid in acetonitrile were used as mobile phase A and B, respectively. The separation gradient was as follows: hold at 0 % B for 0.5 min, 0 to 95 % B for 5 min, 95 % B for 1 min, and 95 to 0 % B for 0.5 min, then hold at 0 % B for 2.5 min. LC flow was 500 μL/min, and column temperature was kept at 50 ℃. Multiple reactions monitoring (MRM) was used in positive ion mode, and the extracted ion chromatogram (EIC) corresponding to the specific transition for each amino acid was used for quantitation. Calibration range was generally 1 nM - 100 μM with $R^2 > 0.99$. Data analysis was performed by using Analyst 1.7 software.

II-14. Statistics

Statistical analyses were performed using IBM SPSS v. 21.0 (IBM Corp., Armonk, NY, USA). AST, ALT, RE, LMR, $T1_{post}$, $\Delta T1$, percentage of necrotic area, Bcl-2/GAPDH, Bax/GAPDH, and C-cas3/GAPDH values were compared among the groups using a one-way analysis of variance with Tukey's post-hoc test. Statistical significance was set at $P < 0.05$.

III. Results

III-1. Animal modeling

Changes in the color of the median and left lobes of the liver were visually assessed, using the color of non-ischemic lobes as reference, in rats with induced IR (control group rats injected with the vehicle only and TMF group rats treated with 6,2',4'-trimethoxyflavone [TMF] 10 min after ischemia). All the rats included in the study survived surgery and the follow-up period (including sham group rats: no IR modeling or vehicle injection).

III-2. MRI-based liver function indices

The signal intensities (Sis) of the liver in T1-weighted gradient echo images (Wis) obtained 3 and 24 h after reperfusion were higher in all three rat groups 20 min after the administration of Gd-EOB-DTPA than before the administration of this compound (Fig. 1A). Conversely, the T1 values of the liver in the T1 maps were lower in all three groups 20 min after the administration of Gd-EOB-DTPA than before. The relative enhancement (RE) values were significantly higher in the control group than in the sham group 24 h after reperfusion ($P < 0.01$; Fig. 1B), whereas the RE values were significantly lower in the TMF group than in the control group 3 and 24 h after reperfusion ($P < 0.05$ and $P < 0.001$, respectively). In addition, the $\Delta T1$ values were significantly higher in the TMF group than in the sham group 3 h after reperfusion and significantly higher in the control group than in the sham group 24 h after reperfusion ($P < 0.001$). In contrast, the $\Delta T1$ values were significantly lower in the TMF group than in the control group 24 h after reperfusion ($P < 0.01$). However, there were no significant differences in the liver-to-muscle ratio (LMR) or $T1\text{-}_{post}$ values among the sham, control, and TMF groups ($P > 0.05$).

III-3. Changes in serum alanine aminotransferase (ALT) and aspartate aminotransferase (AST) levels

Compared to the sham group, the control and TMF groups had significantly higher serum ALT and AST levels at 3 and 24 h after reperfusion ($P < 0.05$, Fig. 2A, B). However, serum ALT levels were significantly lower in the TMF group than in the control group 3 ($P < 0.001$) and 24 h ($P < 0.01$) after reperfusion. Although, serum AST levels were significantly lower in the TMF group than in the control group 3 h after reperfusion ($P < 0.001$), no significant differences were observed between the control and TMF groups 24 after reperfusion ($P = 0.422$).

III-4. Reduction of liver necrotic area by TMF treatment

Extensive hepatocellular necrosis was observed in the control and TMF groups 24 h after reperfusion (Fig. 2C), and no liver necrosis was observed in the sham group. However, the percentage of necrotic areas was significantly lower in

the liver of the rats of the TMF group than in that of the rats of the control group (Fig. 2D).

III-5. Alleviation of apoptosis due to TMF treatment

Terminal deoxynucleotidyl transferase-mediated dUTP nick-end labeling (TUNEL)-positive cells (round brown nuclei) were mainly observed in the control and TMF groups and rarely in the sham group (Fig. 3A). We quantified the expression of the apoptosis-associated proteins Bcl-2, Bax, and cleaved caspase-3 (C-cas3) in liver tissues (Fig. 3B and Supplementary Fig. 1) and found that Bcl-2 protein levels were significantly lower in the control and TMF groups than in the sham group ($P < 0.001$); however, there was no significant difference between the Bcl-2 levels of the control and TMF groups ($P = 0.979$). In contrast, Bax protein expression was significantly higher in the control group than in the sham ($P < 0.01$) and TMF ($P < 0.05$) groups. The expression of the C-cas3 protein in the control group was also significantly higher than that in the sham ($P < 0.01$) and TMF ($P < 0.01$) groups.

III-6. Suppression of AhR expression by TMF administration

AhR expression was mainly observed in the control and TMF groups but rarely in the sham group (Fig. 4A). Therefore, AhR protein levels in liver tissues were significantly higher in the control and TMF groups than in the sham group (Fig. 4B and Supplementary Fig. 2, $P < 0.01$). Notably, the TMF group showed significant lower levels of AhR than the control group ($P < 0.05$).

III-7. Alteration in RNA levels of CYP1a1, CYP1b1, AhRR

AhR targeted genes as CYP1a1, CYP1b1, AhRR were quantified with qRT PCR in liver tissues (Fig. 4C). The CYP1a1 was significantly higher in the control group than in the sham ($P < 0.01$) and TMF groups ($P < 0.01$). The CYP1b1 significantly increased in the control group than sham ($P < 0.001$) and TMF groups ($P < 0.001$). The AhRR significantly increased in the control group than sham group ($P < 0.01$), but no significant differences in the control and TMF groups.

To quantify the expression of enzymes involved in metabolism of tryptophan, TDO, IDO1 and 2 were measured (Fig. 5A). The TDO showed a significant increase in control group ($P < 0.01$) than sham group and significantly decreased in the TMF group ($P < 0.05$) than in the control group. Both IDO1 and 2 were significantly higher in the control ($P < 0.001$) and TMF groups ($P < 0.01$) than sham group, but the IDO2 was no significant difference between the control and TMF groups.

III-8. Variation in the amount of tryptophan and L-Kyn in Liquid chromatography-tandem mass spectrometry (LC-MS/MS)

The amount of tryptophan and L-Kyn were measured by LC-MS/MS (Fig. 5B). Not only tryptophan and L-Kyn were significant differences in the control group ($P < 0.01$) than sham group, but also the TMF group significantly increased compared with control group ($P < 0.05$).

IV. Discussion

In this study, we assessed the hepatoprotective effects of an AhR antagonists on hepatic IR injury in rats. Rats treated with TMF 10 min after ischemia had lower RE values and serum ALT and AST levels than control rats 3 h after reperfusion. Besides, TMF-treated rats had lower RE values, ΔT1 values, serum ALT levels, and necrotic area percentage than control rats 24 h after reperfusion. In addition, the expression of the apoptosis-related proteins Bax and cleaved C-cas3 was lower in TMF-treated rats than in control rats. These results suggest that AhR activation inhibition after ischemia reduces hepatic IR injury.

Under normal conditions, AhR remains inactive in the cytoplasm; it is activated by endogenous or exogenous ligands, such as L-Kyn[10] and 2,3,7,8-tetrachlorodibenzo-*p*-dioxin,[14] respectively. Recently, L-Kyn was found to accumulate in the brain during ischemia and induce the activation of AhR, exacerbating neuronal damage even after reperfusion.[10] Because a significant amount of L-Kyn is produced by tryptophan metabolism in the presence of TDO, phenomena similar to those that occur in the brain after ischemia are likely to occur in the liver as well.[13] However, to the best of our knowledge, these phenomena have not yet been studied. Here, we investigated, for the first time, whether the presence of an AhR antagonist after ischemia affected IR-induced liver damage. Our results showed that the presence of an AhR antagonist inhibited the progression of apoptosis and necrosis in the liver, suggesting that, after ischemia, L-Kyn accumulates in the liver (as in the brain) and activates AhR, possibly leading to hepatic IR injury. However, in the present study, the L-Kyn accumulation and AhR activation inhibition due to L-Kyn accumulation were not studied. Therefore, further investigation is needed.

The present study showed the inhibitory effect of an AhR antagonists on liver cell apoptosis in rats after ischemia. However, most of the pathways that mediate hepatic IR injury after AhR activation still need to be elucidated. Several studies have reported that AhR inhibition reduces neuronal cell death and neurotoxicity.[15,16] In particular, cAMP response element-binding protein (CREB) signaling has been reported to be one of the downstream pathways induced by AhR activation.[10] The report suggests that the activation of AhR due to brain ischemia alters CREB protein-dependent signaling and aggravates brain damage. Given that AhR likely functions via various submechanisms, further investigation on these submechanisms, including CREB signaling changes due to AhR activation in the liver, are needed.

Elevated concentrations of ALT and AST in the serum are representative of hepatocellular injury or necrosis[17,18] because these transferases are leaked from hepatocytes into the blood when such liver cell damages occur.[19] Therefore, we

measured ALT and AST concentration changes to evaluate hepatic injury due to IR. In this study, all rats with IR had higher concentrations of ALT and AST in serum, 3 and 24 h after reperfusion, than rats from the sham group. However, the rats from the TMF group had lower serum ALT and AST levels, 3 and 24 h after reperfusion, than the control rats. These results indicate that TMF administration after ischemia alleviated IR-induced hepatocellular injury and necrosis. Furthermore, histological analyses revealed that TMF rat livers had similar necrotic patterns (though smaller in area percentage) than those of control rats. However, the mechanisms that underlie AhR activation and necrosis have not been elucidated here.

We analyzed the changes in liver function due to IR using Gd-EOB-DTPA, a paramagnetic hepatobiliary magnetic resonance (MR) contrast agent. Several reports have shown that Gd-EOB-DTPA-enhanced MRI is suitable for evaluating liver function because of its organic anion transporting polypeptide (OATP1B1/B3)-dependent hepatocyte-specific uptake and paramagnetic properties.[20,21] In addition, several reports demonstrated the effectiveness of liver function assessment using the SI-based indices of T1-WIs and T1 relaxometry.[22,23] It has previously been show that RE and LMR values are highly correlated with liver function and SI-based indices.[24] RE values were decreased in TMF-treated rats 3 and 24 h after reperfusion compared to those in control group rats. These results suggest that liver function improved in the TMF group. Regarding T1 relaxometry, we determined $T1_{post}$ and $\Delta T1$ values[22,24] and found that, 24 h after reperfusion, the rats from the TMF group had decreased $\Delta T1$ values compared to those of the rats of the control group. These results indicate that liver function improved in TMF-treated rats.

This study has two limitations. First, we only tested a single dose of TMF (5 mg/kg); this dose had previously been suggested by Cuartero *et al*. and Kwon *et al*.[10,12] Given that the concentration of TMF in the blood may vary with the amount of administered TMF, the effect of this molecule on hepatic IR injury may also change. Further studies are required to determine the optimal TMF concentration for reducing hepatic IR injury to its minimum. Second, we only determined AhR expression 24 h after reperfusion and noticed that it was significantly higher in control group rats than in the rats of the sham and TMF groups. These results suggest that elevated AhR expression levels may play an important role in the progression of hepatic IR injury. However, as previously stated, the change in AhR expression was only observed 24 h after reperfusion; therefore, the kinetics of AhR expression after reperfusion was not determined. Additional studies are needed to identify the optimal timing for TMF administration by tracking the changes in AhR expression after reperfusion.

Our findings demonstrate that the administration of AhR antagonists after ischemia has hepatoprotective effects that ameliorate hepatic IR injury. We propose that AhR antagonists could be used for developing new therapeutic approaches for

treating hepatic IR injury. Nevertheless, further studies are needed to elucidate the mechanisms underlying the hepatoprotective effect and to assess the potential clinical applications of AhR antagonist administration.

Figures and Tables

Figure 1

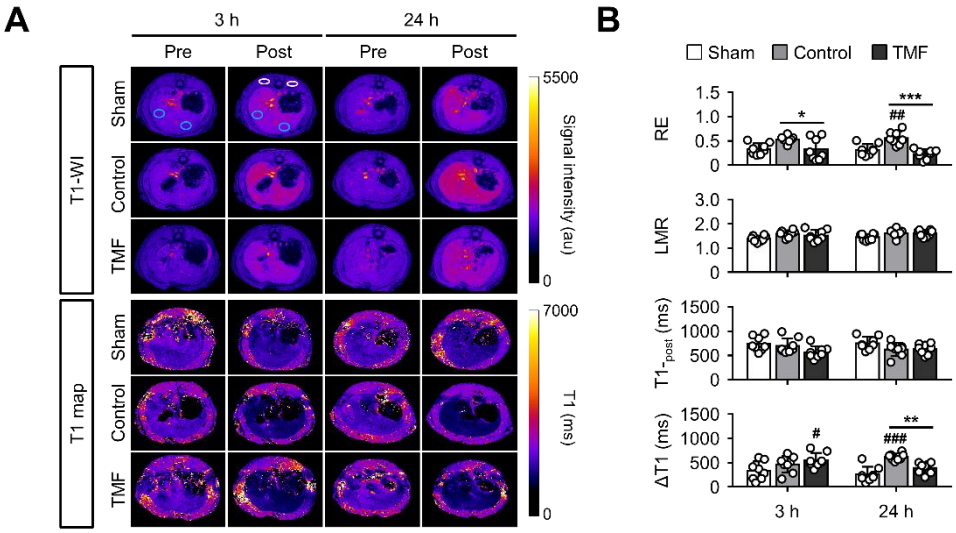

Figure 1. Effect of 6,2',4'-trimethoxyflavone (TMF) treatment on magnetic resonance imaging-based liver function indices. (A) Representative T1-weighted gradient echo images and T1 maps 3 and 24 h after reperfusion. Mean signal intensity (SI) and T1 values of the liver are represented by blue circles, and mean SI values of the paravertebral muscle are represented by white circles. (B) The relative enhancement (RE) values were significantly higher in the control group than in the sham group 24 h after reperfusion. In contrast, 3 and 24 h after reperfusion, the RE values were significantly lower in the TMF group than in the control group. The ΔT1 values were significantly higher in the TMF group than in the sham group 3 h after reperfusion, whereas the ΔT1 values were significantly higher in the control group than in the sham group and significantly lower in the TMF group than in the control group 24 h after reperfusion. Data represent the mean ± standard deviation (n = 8 rats per group). # $P < 0.05$ vs. sham group; ## $P < 0.01$ vs. sham group; ### $P < 0.001$ vs. sham group; * $P < 0.05$ vs. control group; ** $P < 0.01$ vs. control group; *** $P < 0.001$ vs. control group.

Figure 2

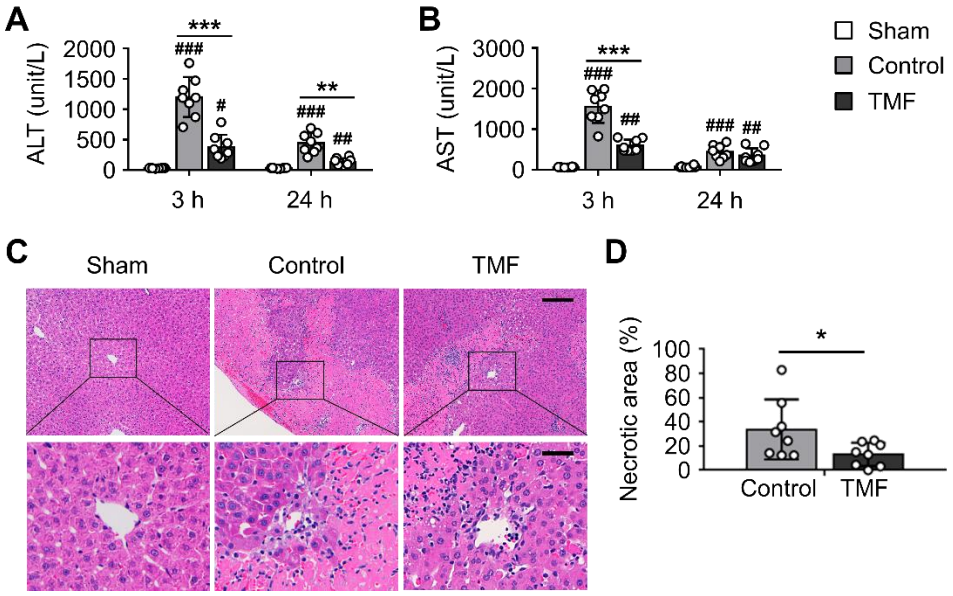

Figure 2. Changes in the concentration of alanine aminotransferase (ALT) and aspartate aminotransferase (AST) in serum and in total necrotic area in the liver after TMF treatment. (A) The control and TMF groups showed significantly higher serum ALT levels than the sham group 3 and 24 h after reperfusion, and serum ALT levels were significantly lower in the TMF group than in the control group 3 and 24 h after reperfusion. (B) The control and TMF groups showed significantly higher serum AST levels than the sham group 3 and 24 h after reperfusion, and serum AST levels were significantly lower in the TMF group than in the control group 3 h after reperfusion. (C) Representative photomicrographs of liver samples, 24 h after reperfusion, stained with H&E (magnification: 50×, scale bar = 200 μm). Enlarged versions of the boxed areas are depicted in the lower panels (scale bar = 50 μm). (D) The necrotic area (%) of the liver of rats of the TMF group was significantly smaller than that of rats of the control group. Data represent the mean ± standard deviation (n = 8 rats per group). # $P < 0.05$ vs. sham group; ## $P < 0.01$ vs. sham group; ### $P < 0.001$ vs. sham group; * $P < 0.05$ vs. control group; ** $P < 0.01$ vs. control group; *** $P < 0.001$ vs. control group.

Figure 3

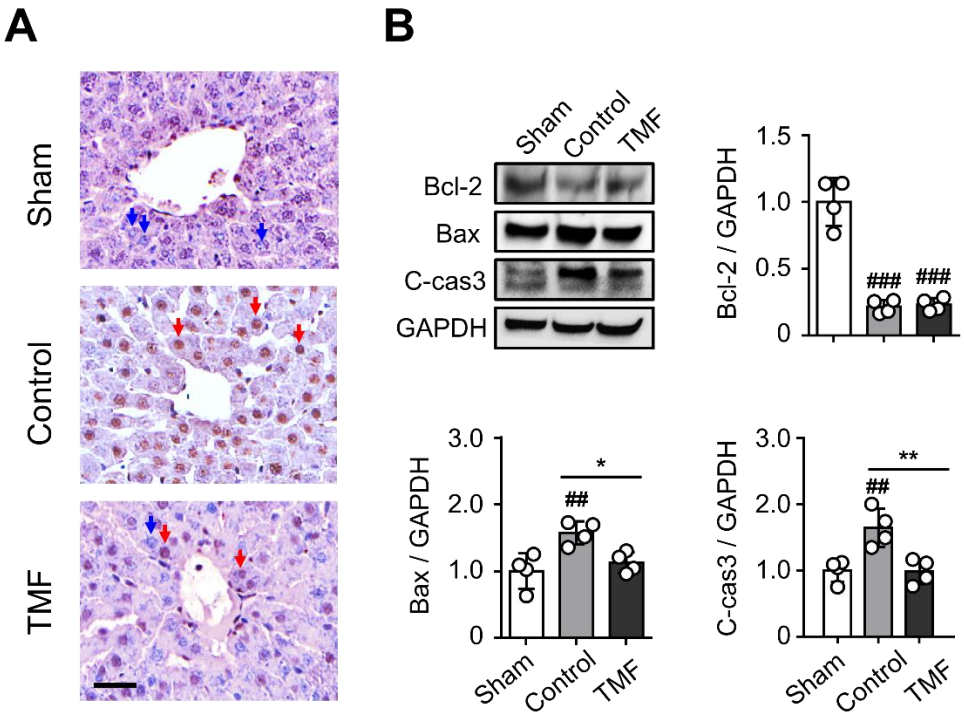

Figure 3. TMF treatment leads to reduced liver cell apoptosis. (A) Representative photomicrographs of terminal deoxynucleotidyl transferase-mediated dUTP nick-end labeling (TUNEL) staining 24 h after reperfusion (magnification: 200×, scale bar = 50 μm). Red arrows, apoptotic cells; blue arrows, viable cells. (B) Bcl-2 expression was significantly lower in the control and TMF groups than in the sham group. Bax and C-cas3 expression in the control group was significantly higher than in the sham and TMF groups. Data represent the mean ± standard deviation (n = 8 rats per group). $^{\#\#}$ P < 0.01 vs. sham group; $^{\#\#\#}$ P < 0.001 vs. sham group; * P < 0.05 vs. control group; ** P < 0.01 vs. control group. Full-length blots/gels are presented in Supplementary Figure 1.

Figure 4

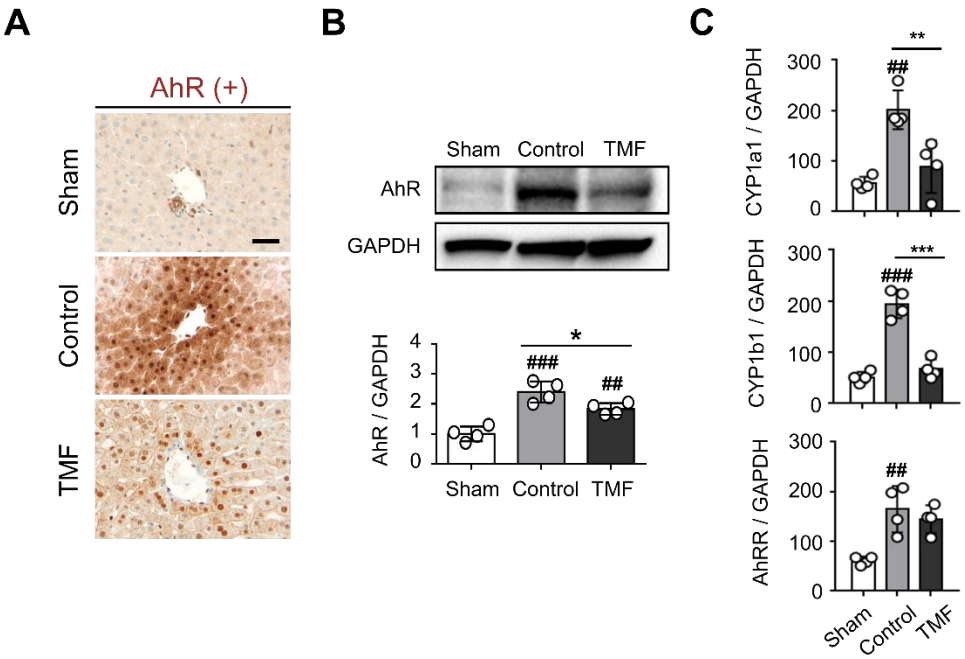

Figure 4. TMF treatment suppresses aryl hydrocarbon receptor (AhR) expression and changes in target genes of AhR. (A) Representative photomicrographs showing stained AhR 24 h after reperfusion (magnification: 200×, scale bar = 50 μm). (B) AhR protein concentrations were significantly higher in the control and TMF groups than in the sham group. The TMF group showed significantly lower concentrations of AhR than the control group. Data represent the mean ± standard deviation (n = 8 rats per group). $^{\#\#}$ P < 0.01 vs. sham group; $^{\#\#\#}$ P < 0.001 vs. sham group; $^{\#}$ P < 0.05 vs. control group. Full-length blots/gels are presented in Supplementary Figure 2. (C) RNA expressions of CYP1a1, CYP1b1 and AhRR. The genes were significantly higher in the control and TMF groups than in the sham group. The TMF group was significantly lower in CYP1a1 and CYP1b1 than the control group. Data are represented as means ± standard deviations (n = four rats in each group). $^{\#\#}$ P < 0.01 vs. sham group; $^{\#\#\#}$ P < 0.001 vs. sham group; ** P < 0.01 vs. control group; *** P < 0.001 vs. control group.

Figure 5

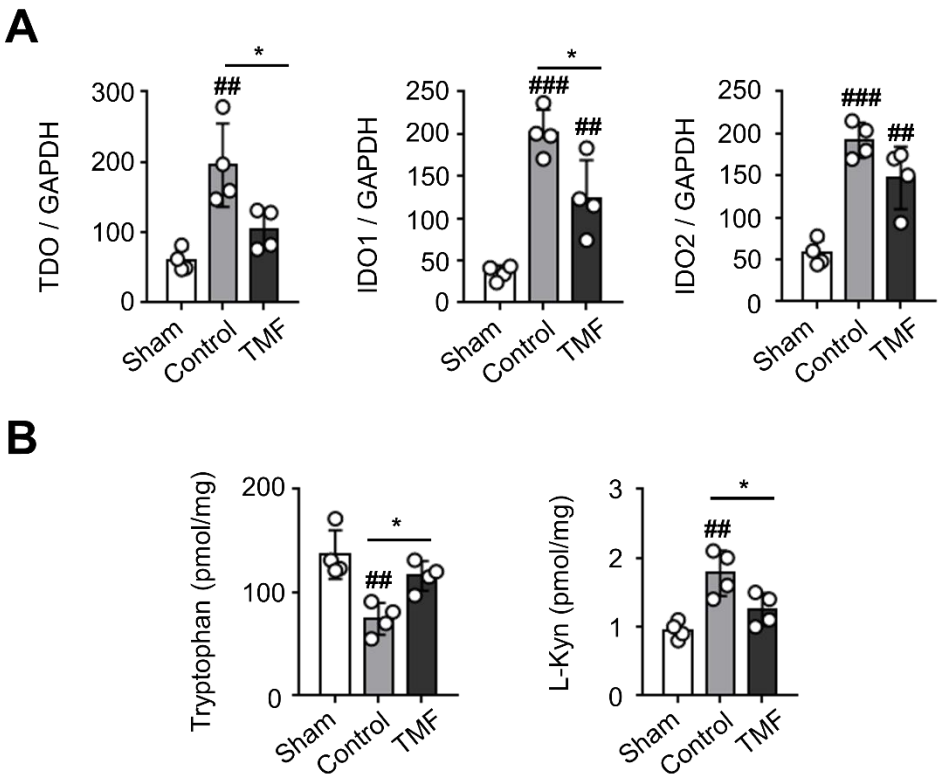

Figure 5. Alteration in RNA expression of tryptophan metabolic enzymes and changes in amount of Tryptophan-derived L-kynurenine (L-Kyn) after 6,2',4'-trimethoxyflavone (TMF) administration (A) The control group were significantly higher RNA expression of TDO than sham group. The TMF group was significantly lower than control group. Both IDO1 and 2 levels were significantly higher in the control and TMF groups than sham group, but only IDO1 expression was significantly lower in the TMF group than control group. (B) The amount of tryptophan and L-Kyn in liquid chromatography-tandem mass spectrometry (LC-MS/MS). The tryptophan was significantly lower in the control group than sham group. The TMF group was significantly higher than control group. The amount of the L-Kyn was significantly higher in the control group than sham group, as well as significantly lower in the TMF group than control group. Data are represented as means ± standard deviations (n = four rats in each group). $^{\#\#}$ $P < 0.01$ vs. sham group; * $P < 0.05$ vs. control group.

Figure 6

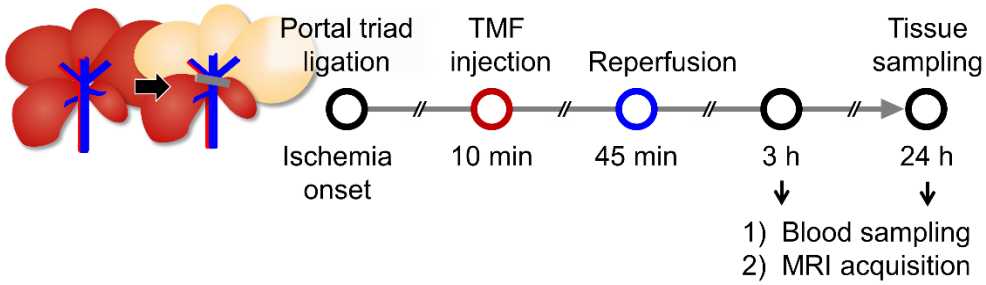

Figure 6. Schematic diagram of the experimental procedure. Hepatic ischemia was induced by clamping the portal triad for 45 min, followed by reperfusion. TMF was administered 10 min after ischemia. Blood samples and magnetic resonance imaging data were obtained 3 and 24 h after reperfusion. Liver tissues were harvested 24 h after reperfusion.

Supplementary Figure 1. The full-length blots/gels including the key data presented in Fig. 3.

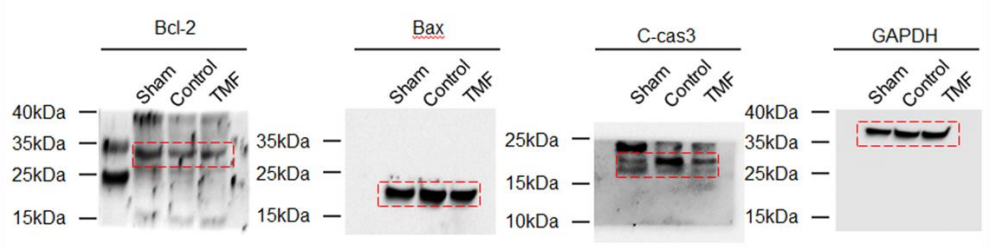

Supplementary Figure 2. The full-length blots/gels including the key data presented in Fig. 4.

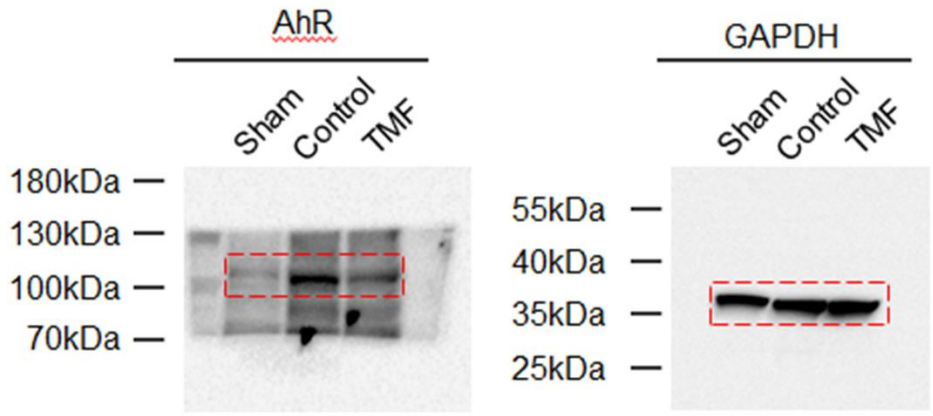

Supplementary Table S1. MRI sequence parameters

	T1-WI	**T1 map**
TR (ms)	15.46	4.9
TE (ms)	2.73	2.47
Inversion time (ms)	-	100/209/437/915/4000
FA	20	5
Matrix	128 × 128	96 × 96
FOV (mm)	50	70
Slice thickness (mm)	2	2
Slice number	1	1
Gap (mm)	0	0

Supplementary Table S2. qRT PCR primer list

1) AhRR – Forward 5′ GCCTCAATACAGAGCTGGACC 3′,
Reverse 5′ TGAGGCGAAGGACTGAAAGT 3′;

2) CYP1a1 – Forward 5′ GCTTTGGCAGACGTTATGACC 3′,
Reverse 5′ TGTCGGAAGGTCTCCAGGAT 3′;

3) CYP1b1 – Forward 5′ GCCTTAGTGCAGACAGTCCA 3′,
Reverse 5′ CCAGGACCGAAACGAGTAGC 3′;

4) IDO1 – Forward 5′ GCACTGGAGAAGGCACTGTGTAG 3′,
Reverse 5′ GATCCACGAAGTCACGCATCCTC 3′;

5) IDO2 – Forward 5′ TAACGAGTTACCGCGAGCAG 3′,
Reverse 5′ TAATCACAGGAAGTCGGGACG 3′;

6) TDO – Forward 5′ ATCGTGTGGTGGTCATCTTCAAGC 3′,
Reverse 5′ AGCCGGAACTGTAGACTCTGGAAG 3′;

References

1 Kokudo, N., Takemura, N., Ito, K. & Mihara, F. The history of liver surgery: Achievements over the past 50 years. *Ann Gastroenterol Surg* **4**, 109-117, doi:10.1002/ags3.12322 (2020).

2 Orci, L. A. *et al.* The role of hepatic ischemia-reperfusion injury and liver parenchymal quality on cancer recurrence. *Dig Dis Sci* **59**, 2058-2068, doi:10.1007/s10620-014-3182-7 (2014).

3 Yamazaki, S. & Takayama, T. Current topics in liver surgery. *Ann Gastroenterol Surg* **3**, 146-159, doi:10.1002/ags3.12233 (2019).

4 Zabala, V. *et al.* Transcriptional changes during hepatic ischemia-reperfusion in the rat. *PLoS One* **14**, e0227038, doi:10.1371/journal.pone.0227038 (2019).

5 Bi, J. *et al.* Irisin alleviates liver ischemia-reperfusion injury by inhibiting excessive mitochondrial fission, promoting mitochondrial biogenesis and decreasing oxidative stress. *Redox Biol* **20**, 296-306, doi:10.1016/j.redox.2018.10.019 (2019).

6 Guan, L. Y. *et al.* Mechanisms of hepatic ischemia-reperfusion injury and protective effects of nitric oxide. *World J Gastrointest Surg* **6**, 122-128, doi:10.4240/wjgs.v6.i7.122 (2014).

7 Opitz, C. A. *et al.* An endogenous tumour-promoting ligand of the human aryl hydrocarbon receptor. *Nature* **478**, 197-203, doi:10.1038/nature10491 (2011).

8 Denison, M. S. & Nagy, S. R. Activation of the aryl hydrocarbon receptor by structurally diverse exogenous and endogenous chemicals. *Annu Rev Pharmacol Toxicol* **43**, 309-334, doi:10.1146/annurev.pharmtox.43.100901.135828 (2003).

9 Hankinson, O. The aryl hydrocarbon receptor complex. *Annu Rev Pharmacol Toxicol* **35**, 307-340, doi:10.1146/annurev.pa.35.040195.001515 (1995).

10 Cuartero, M. I. *et al.* L-kynurenine/aryl hydrocarbon receptor pathway mediates brain damage after experimental stroke. *Circulation* **130**, 2040-2051, doi:10.1161/CIRCULATIONAHA.114.011394 (2014).

11 Padmanabhan, A. & Haldar, S. M. Neuroprotection in ischemic stroke: AhR we making progress? *Circulation* **130**, 2002-2004, doi:10.1161/CIRCULATIONAHA.114.013533 (2014).

12 Kwon, J. I. *et al.* Aryl hydrocarbon receptor antagonism before reperfusion attenuates cerebral ischaemia/reperfusion injury in rats. *Sci Rep* **10**, 14906, doi:10.1038/s41598-020-72023-5 (2020).

13 Green, A. R., Woods, H. F. & Joseph, M. H. Tryptophan metabolism in the isolated perfused liver of the rat: effects of tryptophan concentration, hydrocortisone and allopurinol on tryptophan pyrrolase activity and kynurenine formation. *Br J Pharmacol* **57**, 103-114, doi:10.1111/j.1476-5381.1976.tb07660.x (1976).

14 Quintana, F. J. *et al.* Control of T(reg) and T(H)17 cell differentiation by the aryl hydrocarbon receptor. *Nature* **453**, 65-71, doi:10.1038/nature06880 (2008).

15 Kajta, M., Wojtowicz, A. K., Mackowiak, M. & Lason, W. Aryl hydrocarbon

receptor-mediated apoptosis of neuronal cells: a possible interaction with estrogen receptor signaling. *Neuroscience* **158**, 811-822, doi:10.1016/j.neuroscience.2008.10.045 (2009).

16 Sanchez-Martin, F. J., Fernandez-Salguero, P. M. & Merino, J. M. Aryl hydrocarbon receptor-dependent induction of apoptosis by 2,3,7,8-tetrachlorodibenzo-p-dioxin in cerebellar granule cells from mouse. *J Neurochem* **118**, 153-162, doi:10.1111/j.1471-4159.2011.07291.x (2011).

17 Jo, K. M. *et al.* Serum Aminotransferase Level in Rhabdomyolysis according to Concurrent Liver Disease. *Korean J Gastroenterol* **74**, 205-211, doi:10.4166/kjg.2019.74.4.205 (2019).

18 Giboney, P. T. Mildly elevated liver transaminase levels in the asymptomatic patient (vol 71, pg 1105, 2005). *American Family Physician* **72**, 41-41 (2005).

19 Young, T. H. *et al.* Quantitative rat liver function test by galactose single point method. *Lab Anim* **42**, 495-504, doi:10.1258/la.2007.06040e (2008).

20 Meier, P. J., Eckhardt, U., Schroeder, A., Hagenbuch, B. & Stieger, B. Substrate specificity of sinusoidal bile acid and organic anion uptake systems in rat and human liver. *Hepatology* **26**, 1667-1677, doi:10.1002/hep.510260641 (1997).

21 Nassif, A. *et al.* Visualization of hepatic uptake transporter function in healthy subjects by using gadoxetic acid-enhanced MR imaging. *Radiology* **264**, 741-750, doi:10.1148/radiol.12112061 (2012).

22 Ma, C. *et al.* The hepatocyte phase of Gd-EOB-DTPA-enhanced MRI in the evaluation of hepatic fibrosis and early liver cirrhosis in a rat model: an experimental study. *Life Sci* **108**, 104-108, doi:10.1016/j.lfs.2014.05.016 (2014).

23 Haimerl, M. *et al.* Gd-EOB-DTPA-enhanced MRI for evaluation of liver function: Comparison between signal-intensity-based indices and T1 relaxometry. *Sci Rep* **7**, 43347, doi:10.1038/srep43347 (2017).

24 Nakagawa, M. *et al.* Measuring hepatic functional reserve using T1 mapping of Gd-EOB-DTPA enhanced 3T MR imaging: A preliminary study comparing with (99m)Tc GSA scintigraphy and signal intensity based parameters. *Eur J Radiol* **92**, 116-123, doi:10.1016/j.ejrad.2017.05.011 (2017).

25 Karatzas, T., Neri, A. A., Baibaki, M. E. & Dontas, I. A. Rodent models of hepatic ischemia-reperfusion injury: time and percentage-related pathophysiological mechanisms. *J Surg Res* **191**, 399-412, doi:10.1016/j.jss.2014.06.024 (2014).

26 Bae, U. J. *et al.* SPA0355 attenuates ischemia/reperfusion-induced liver injury in mice. *Exp Mol Med* **46**, e109, doi:10.1038/emm.2014.48 (2014).

국문요약

Aryl hydrocarbon receptor (AhRs)는 뇌 허혈성 손상의 중요한 매개체이다. 허혈 후 AhR 활성화의 약리학적 억제는 뇌 허혈/재관류(ischemia/reperfusion, IR) 손상을 완화한다. 본 연구에서는 허혈 후 AhR 길항제를 투여하는 것이 간 IR 손상을 완화할 수 있는지 조사하였다. 쥐에서 70% 부분 간 IR 손상 (45분 허혈 후 24시간 재관류)을 유도하였고, 허혈 후 10분 째에 6, 2', 4'-trimethoxyflavone (TMF; 5mg/kg)을 복강 투여하였다. 혈청, 자기공명영상 기반 간 기능 지수 및 간 조직을 이용하여 간 IR 손상을 평가했다. TMF 투여군은 재관류 후 3시간 째에 대조군 보다 relative enhancement (RE) 값과 alanine aminotransferase (ALT) 및 aspartate aminotransferase level이 유의하게 낮았다. 또한, 재관류 후 24시간 째에 TMF 투여군은 대조군 보다 RE, ΔT1, ALT, 괴사 면적 비율, 세포 자멸 관련 단백질 Bax와 cleaved caspase-3의 발현이 TMF 투여군에서 유의하게 낮았다. 따라서, 본 연구는 허혈 후 AhR 활성화 억제가 IR 유도된 간 손상을 개선하는 것을 시사한다.

중심단어: Aryl hydrocarbon receptor, 간 허혈/재관류 손상, 자기공명영상